

Temperature dependences of flux creep and critical current in molybdenum sulfides

A. V. Mitin

Institute for Physical Problems, Academy of Sciences of the USSR

(Submitted 16 June 1986)

Zh. Eksp. Teor. Fiz. **93**, 590–604 (August 1987)

Results are presented of an investigation of the temperature ($T > 0.5$ K) dependence of the decay rate of the “frozen-in” magnetic field $H_i \gg H_{c1}$ (flux creep) and of the critical current density J_c for polycrystalline ternary molybdenum sulfides containing lead, tin, and copper. In all the specimens, for which J_c (at 10 kOe and 4.2 K) was greater than 10^4 A/cm², H_i was found to decay logarithmically (except for initial times $t < 20$ s), in agreement with the predictions of the Anderson theory, which assumes a thermal activation mechanism for vortex diffusion. However, it is found that thermal activation alone does not explain the observed weak dependence of the flux creep rate on the temperature, nor the abrupt change in the slope of $J_c(T)$ at temperatures 2–3 degrees Kelvin below the critical point T_c . A satisfactory explanation of these results is obtained using a model that allows for possible quantum diffusion of vortices in addition to thermal activation.

INTRODUCTION

In addition to their very high second critical fields $H_{c2}(0) = 300\text{--}600$ kOe (Refs. 1–3), ternary molybdenum sulfides containing tin and lead have high critical current densities J_c (140 kOe, 4.2 K) $> 10^4$ A/cm² (Refs. 4–8). Highly reproducible results⁵ have been obtained using bulk specimens instead of thin-film coatings,^{9–11} because the composition and preparation conditions can be controlled more precisely. Remote-sensing methods are used to measure J_c in bulk specimens in order to eliminate contact effects, which are especially pronounced for $T > 4.2$ K.

According to present theory, vortex pinning by various types of structural inhomogeneities is responsible for the lack of appreciable energy dissipation during the flow of very high currents in type-II superconductors in magnetic fields $H_{c1} < H < H_{c2}$. The current density in the superconductor is assumed¹² to reach the critical value J_c when the Lorentz forces acting on the vortices become comparable to the pinning forces.

Anderson¹² predicted that J_c , and hence the “frozen-in” magnetic field in a type-II superconductor, should decay logarithmically with time (this is called flux creep), because in some cases the thermal energy of a vortex may overcome the pinning forces confining it in a potential well near a pinning center. The latter are generally defects in the superconductor, such as inclusion of secondary phases, pores, dislocations, strain, etc. Anderson’s prediction was borne out in the experiments of Kim and co-workers,¹³ who studied the time dependence of the magnetic flux frozen into hollow tubes of Nb-Zr alloy. Thermal activation of vortex diffusion also explains why J_c is so sensitive to T at low temperatures.

While subsequent work^{14–22} appears to support the basic assumptions of the Anderson theory,¹² direct experimental confirmation of thermally activated flux creep is lacking. At the same time, convincing alternative explanations have not been developed.

In this paper we report data from measurements of flux creep and critical current as functions of temperature. We show that quantum diffusion of vortices as well as thermal activation must be treated in order to explain the data.

EXPERIMENT

Ternary molybdenum sulfide crystals containing lead, tin, and copper were synthesized under the same conditions as in Refs. 5, 23. The resulting compounds were carefully ground in an agate mortar and pressed in cylindrical dies at a pressure of 10–15 kbar. After pressing, the specimens were rendered homogeneous by annealing them for 24 h. Specimens with differing microstructures were obtained, depending on the annealing temperature $700^\circ\text{C} < T_a < 1200^\circ\text{C}$. A Geigerflex diffractometer (Cu K_α radiation, $\lambda = 1.541$ Å) was used to analyze the phase composition of the annealed specimens.

The specimens were shaped by mechanical treatment into tubes of outer diameter $a = 5$ mm, height $h = 15\text{--}20$ mm, and wall thickness $w = 1.2\text{--}1.5$ mm. The values J_c were found from the difference between the magnetic fields inside and outside the specimen (the same method was employed previously^{13,14,24} for alloy specimens). Calibrated bifilar copper resistance coils connected in a bridge circuit served as the magnetic field sensors. The axis of the specimens was aligned parallel to the external magnetic field which, depending on the requirements imposed on the field strength and stability, was generated by a superconducting or by a water-cooled Bitter magnet. Most of the measurements were carried out at the International Laboratory for High Magnetic Fields and Low Temperatures at Wroclaw, Poland.

Figure 1 shows traces of the internal field H_i as a function of the external field H_e for a $\text{Pb}_{1.2}\text{Mo}_{6.4}\text{S}_8$ specimen at two fixed temperatures 1.7 and 4.2 K. The time dependence $H_i(t)$ for fixed T and H_e was found to within 0.05% by a digital voltmeter. For temperatures $T = 1.6\text{--}16$ K the specimens were cooled by liquid or gaseous helium-4. Lower temperatures were achieved by using a cryostat equipped with a pump for evacuating the helium-3 vapor. The flux creep was measured for several hours, during which time the temperature was held constant to within 0.01 K.

RESULTS

The decay rate of the magnetic field (or current) induced in molybdenum sulfides of identical composition

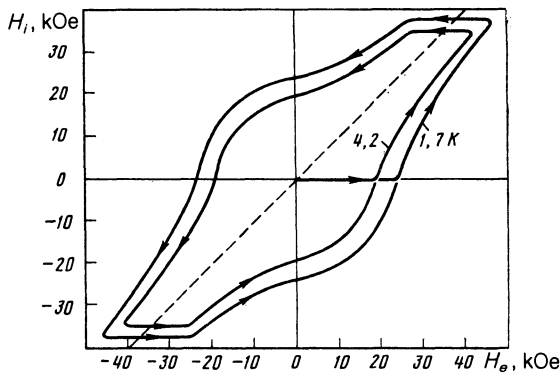


FIG. 1. Field H_i inside a hollow $\text{Pb}_{1.2}\text{Mo}_{6.4}\text{S}_8$ tube annealed at $T_a = 1020^\circ\text{C}$, as a function of the applied external field H_e . Specimen dimensions: outer diameter 5 mm, wall thickness 1.4 mm, height 16 mm.

$\text{Pb}_{1.2}\text{Mo}_{6.4}\text{S}_8$ depends on the annealing temperature T_a and can vary widely.⁵ For example if the decay is characterized by $t_{1/2}$, the time for the current in the specimen to drop by a factor of two, one finds that $t_{1/2}$ ranges from 10^{14} to 10^{500} years, depending on T_a . The slowest decay measured in our experiments was found for the $\text{Pb}_{1.2}\text{Mo}_{6.4}\text{S}_8$ specimen with $T_a = 820^\circ\text{C}$. The x-ray diffraction data indicate that this specimen was rich in secondary phases Mo, MoS_2 , PbS, and Pb (the content was greater than 10%). As T_a increases, the large defects and secondary-phase inclusions break up to form numerous smaller ones, the specimens become more homogeneous, and the current decays more rapidly. Figure 2 shows the relative change in the "frozen" field H_i as a function of time for one of the $\text{Pb}_{1.2}\text{Mo}_{6.4}\text{S}_8$ specimens annealed at 1020°C . These measurements were made at several temperatures 5 s after the field H_e was turned off. We see from Fig. 2 that after the initial period ($t < 20$ s), the curves $H_i(t)$ were logarithmic to within the experimental error. The same behavior was observed for all the other molybdenum sulfides, regardless of composition (including specimens with tin or copper as the third component).

Figure 3 shows the relative decay rate, $[1/H_i(5)] dH_i(t)/d \ln(t/t_0)$ of the field H_i frozen into the specimen as a function of T for $t > t_0 = 20$ s. Taking $T = 4.2$ K, say, as the common reference point, we see that the measured flux creep rates decrease with falling temperature much more slowly than predicted by the Anderson relation¹²

$$\frac{\delta H_i}{H_i} = - \frac{k'w}{H_i(H_i+B_0)} \frac{k_B T}{d^4} \ln(t/t_0) \quad (1)$$

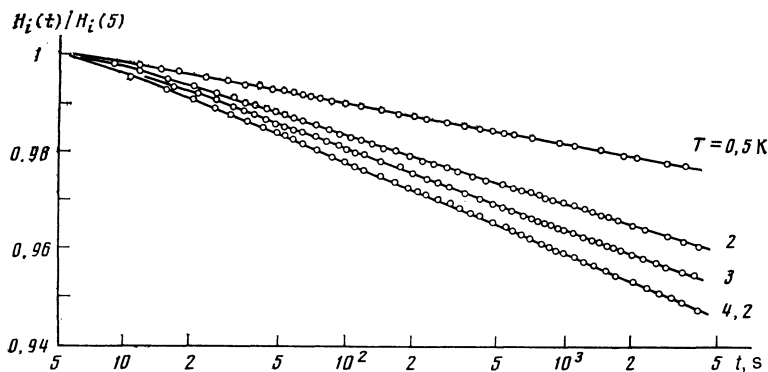


FIG. 2. Relative internal field $H_i(t)/H_i(5)$ versus time t (logarithmic scale) for four fixed temperatures ($H_e = 0$) for a $\text{Pb}_{1.2}\text{Mo}_{6.4}\text{S}_8$ specimen with $T_a = 1020^\circ\text{C}$. $H_i(5)$ is the "frozen" field 5 s after H_e was turned off.

(dashed line). Here $k' = 4\pi$, k_B is Boltzmann's constant, d is the average distance between effective pinning centers (or the mean diameter of the stream of vortex stream), w is the wall thickness of the tubular specimen, and the constant $B_0 = \Phi_0/d_B^2$ determines the slope of the experimental curves J_c for weak fields $H_{c1} < H < 0.1H_{c2}$:

$$J_c = \alpha(T)/(H+B_0), \quad (2)$$

The pinning force density $\alpha(T)$ is independent of H , and Φ_0 is the flux quantum.

Figure 4 plots the normalized reciprocal critical current $J_c(100 \text{ kOe})/J_c(H)$ at $T = 4.2$ K for $\text{Pb}_{1.2}\text{Mo}_{6.4}\text{S}_8$ specimens with different annealing temperatures. We see that for $H_e < 80$ kOe, the data follow Eq. (2) to within the experimental error. As T_a increases from 720 to 1120°C , B_0 rises from 50 to $2.1 \cdot 10^4$ G. Comparison of these data shows that the flux creep is greatest for specimens for which the slope of $J_c(H)$ at weak fields is small. We note that for $T < 4.2$ K, the correction for the temperature dependence of B_0 for our specimens is less than the experimental error. If one uses the value of B_0 for the most homogeneous $\text{Pb}_{1.2}\text{Mo}_{6.4}\text{S}_8$ specimen ($T_a = 1120^\circ\text{C}$) to calculate the parameter $d_B = (\Phi_0/B_0)^{1/2} = 440 \text{ \AA}$, the result agrees reasonably well with the value $d_i = 330 \text{ \AA}$ calculated from (1) with $T = 4.2$ K. For specimens annealed at lower temperatures, these estimates for d_B and d_i may differ by a factor of 1.5–2.5 (Ref. 5).

Figure 5 shows temperature curves $J_c(T)$ for a $\text{Pb}_{1.2}\text{Mo}_{6.4}\text{S}_8$ specimen with $T_a = 1020^\circ\text{C}$ for fixed magnetic fields. An extended linear region at low temperatures $0.05T_c < T < 0.6T_c$ was also observed for the other lead-containing molybdenum sulfides, although their critical current densities varied by more than an order of magnitude.^{5,23} In many cases (e.g., for $\text{Cu}_{1.8}\text{Mo}_6\text{S}_8$), the slope of $J_c(T)$ tended to decrease as T approached zero; a similar decrease was noted for Nb-Zr specimens in Ref. 13.

If the nonlinear portion of $J_c(T)$ is extrapolated to zero critical current, the resulting critical temperature $T_c(J_c \rightarrow 0)|_{H=\text{const}}$ is roughly 2–3 K higher than the value found by extrapolating the straight-line portion.

DISCUSSION

Extended experiments lasting roughly a year indicate that flux creep does not occur in type-I superconductors, and in type-II superconductors it becomes appreciable only for $H > H_{c1}$ (Ref. 15). The flux creep mechanism therefore in all probability involves the penetration of Abrikosov vor-

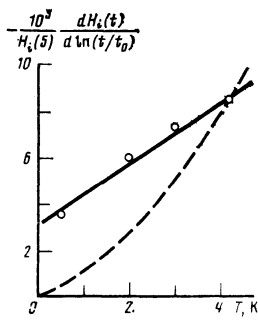


FIG. 3. Temperature dependence of the relative rate of change $- [10^3 / H_i(5)] [dH_i(t)/d \ln(t/t_0)]$ of the "frozen" field H_i in a $\text{Pb}_{1.2}\text{Mo}_{0.4}\text{S}_8$ specimen ($T_a = 1020^\circ\text{C}$). The dashed curve gives the theoretical flux creep rate at $T = 4.2$ K predicted by the Anderson formula.¹²

tex filaments into the superconductor, where they subsequently diffuse.

Our data show that 20 s after the external field is turned off, the "frozen" field $H_i \gg H_{c1}$ decays logarithmically (i.e., just as predicted by the thermal activation model¹²) for all of our specimens, which had large critical currents J_c (10 kOe, 4.2 K) $> 10^4$ A/cm² and Ginzburg-Landau (GL) parameters $\kappa \gg 10$. The initial nonlogarithmic behavior for $t < 20$ s is probably due to the relatively slow relaxation²⁵ to a critical state in thermodynamic equilibrium after the external field is discontinued.

However, examination of the temperature dependence of the flux creep (Fig. 3) reveals that the experimental values of the derivative $|H_i^{-1} dH_i/d \ln(t/t_0)|$ fall off with temperature much more slowly than predicted by (1), and a similar discrepancy is observed for the ternary molybdenum sulfides containing tin or copper. This could be due in part to local heating of the specimen by 2–3 K due, e.g., to the energy liberated when vortices (or even whole streams of vortices) jump across the potential barriers separating adjacent pinning centers. However, this explanation seems implausible because the derivative $|H_i^{-1} dH_i/d \ln(t/t_0)|$ remains constant for t ranging over several decades, during which

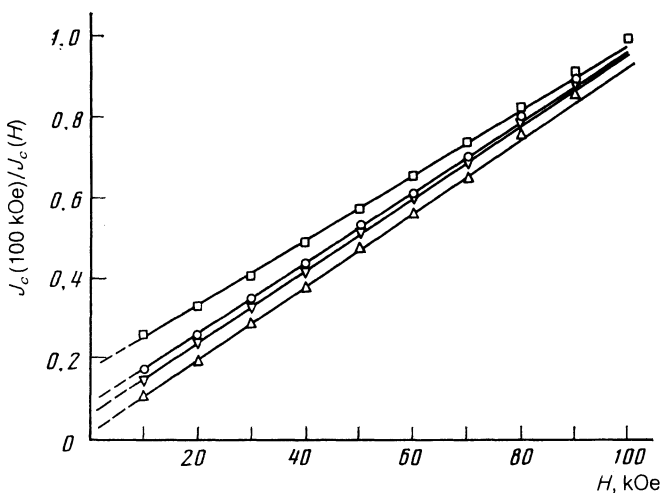


FIG. 4. Normalized reciprocal critical current $J_c(100 \text{ kOe})/J_c(H)$ versus field H at $T = 4.2$ K for $\text{Pb}_{1.2}\text{Mo}_{0.4}\text{S}_8$ specimens annealed at $T_a = 820$ (Δ), 920 (∇), 1020 (\circ), and 1120 (\square) $^\circ\text{C}$.

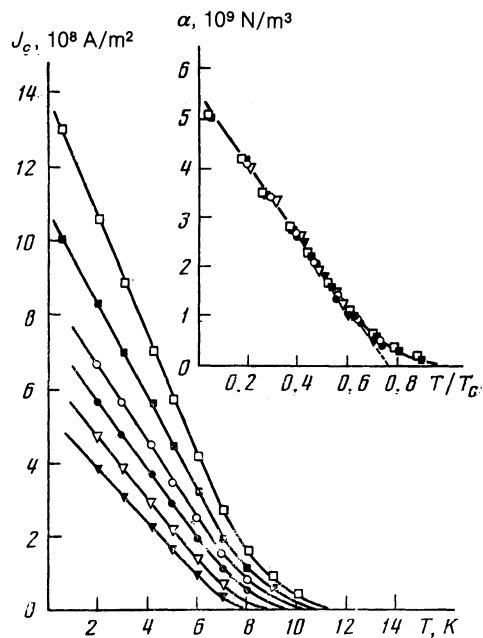


FIG. 5. Temperature curves of critical current density for a $\text{Pb}_{1.2}\text{Mo}_{0.4}\text{S}_8$ specimen with $T_a = 1020^\circ\text{C}$, with second critical field $H_{c2}(T \rightarrow 0) = 460$ kOe, $T_c(H \rightarrow 0) \approx 12.5$ K, $|dH_{c2}/dt|_{T=T_c} = 48$ kOe/k, for fixed magnetic fields 30 (\square), 40 (\blacksquare), 50 (\circ), 60 (\bullet), 80 (∇), and 100 kOe (\blacktriangledown). The insert shows the dependence of the pinning force density parameter $\alpha(T) = (H + B_0) \cdot J_c(T)$ on the reduced temperature. The values $T_c(H)$ were found by extrapolating the nonlinear part of $J_c(T)|_{H=\text{const}}$ to the T/T_c axis.

time the average specific liberated energy drops by several orders of magnitude.

In principle, one could try to explain the slow decay rate of the flux creep with decreasing temperature in terms of spatial variations of the local values of the critical parameters in the superconducting specimen, i.e., its inhomogeneity (produced, e.g., by internal strain, changes in composition, the presence of secondary phases, etc.). In this case, if the inhomogeneities in the superconductor are assumed to be randomly distributed,^{26,27} any transport current J in the superconductor must be accompanied by energy dissipation, which can be assessed in terms of the electric field

$$E = J \rho_n \exp\left(\frac{T - T_c}{T} + \frac{B}{B_*} + \frac{J}{J_*}\right). \quad (3)$$

Here the parameters T_* , B_* , and J_* characterize the width of the superconducting transition; they are assumed to remain nearly constant for T , B , and J varying over a wide range.²⁷ Under our experimental conditions, relation (3) can be used as in Ref. 14 to derive an expression for the time derivative of the frozen-in field:

$$\left| \frac{dH_i}{dt} \right| = \frac{H_i \rho_n}{2\pi a w} \exp[(T - T_c)/T_* + B/B_* + J/J_*], \quad (4)$$

where a and w are the outer radius and wall thickness of the specimen, respectively. If the change in H_i inside the tubular specimen is small and no external field is present ($H_e = 0$), we also have

$$\delta H_i \approx \delta B \approx 4\pi \omega \delta J.$$

Because H_i , and hence B and J , drop by only a few

percent over three decades of time, while the derivative $|dH_i/dt|$ also decreases by a few percent, the change in the latter may be assumed to be due entirely to the change in the argument of the exponential. Relation (4) shows that for specimens with a sharp superconducting transition curve (i.e., small T_* , $B_* = T_* \partial B / \partial T$, and $J_* = T_* \partial J / \partial T$), a given relative change $\delta J / J$ in the induced current retards the flux creep much more than for specimens with a broad transition. These data show, however, that for $t > 20$ s the change in $|dH_i/d \ln(t/t_0)|$ is smallest for the least uniform specimens (with low annealing temperatures); these specimens have a high concentration of secondary phases,⁵ and in general their superconducting transition extends over a wider range of temperatures and magnetic fields than for specimens annealed at higher temperatures. The width of the transition curves, determined by the ordinary four-contact method at measurement current densities $J < 1$ A/cm², corresponded to an increase in the specific electrical conductivity of the specimen from $0.1\rho_n$ to $0.5\rho_n$, where ρ_n is the electrical resistance of the specimen in the normal state near the superconducting transition.

Some of the other data obtained under conditions of low energy dissipation are also difficult to interpret if the inhomogeneities are assumed to be randomly distributed in the superconductor, as in Refs. 26, 27. For instance, for specimens with small $|H_i^{-1} dH_i/d \ln(t/t_0)|$ and hence weak fields $E < 10^{-10}$ V/cm, the curves $J_c(H)$ for $T = \text{const}$ are highly nonlinear and their slope $|\partial J_c / \partial H|$ rises abruptly in the interval 10 kOe $< H < 80$ kOe. This conflicts with Eq. (3), which predicts that $J_c(H)$ should be linear to within 5% when J_c varies by a factor of e .

On the other hand, the distinct correlation between the values B_0 , characterizing the dependence $J_c(H)$, and the values of $|H_i^{-1} dH_i/d \ln(t/t_0)|$ for $\text{Pb}_{1.2}\text{Mo}_{6.4}\text{S}_8$ specimens with different T_a (Ref. 5) strongly supports the activation model for vortex diffusion.¹² From this standpoint, the lack of a definite correlation between the flux creep rate measured for low values $E < 10^{-8}$ V/cm and the transition curves found at $E = 10^{-6}$ V/cm reflects the fact that near the transition to normal conductivity, energy dissipation is due more to viscous vortex flow than to diffusion activation.¹⁴

In the context of the activation mechanism, the weak temperature dependence of the flux creep rate may be explained formally by allowing the parameter d , which is determined by the microstructure of the specimen, to depend on temperature. However, our data cast doubt on the validity of such an assumption because, at least for low temperatures $0.5 \text{ K} \leq T \leq 4.2 \text{ K}$, the values $B_0 = \Phi_0/d_B^2$ deduced from the experimental curves $J_c(H)$ are independent of T to within the 5% experimental error.

The most likely explanation is that thermal activation is accompanied by another mechanism that permits vortex diffusion even at very low temperatures. Such a mechanism might involve the quantum tunneling of local regions of the vortices through the potential barriers separating adjacent pinning centers.⁵ The quantum diffusion mechanism is illustrated schematically in Fig. 6, where three successive positions of a vortex are indicated. Numerous individual quantum hops of this type may occur, with the result that the vortices diffuse as a whole in a direction opposite to the magnetic field gradient $\nabla(B)$ in the specimen ($\langle B \rangle$ is the mag-

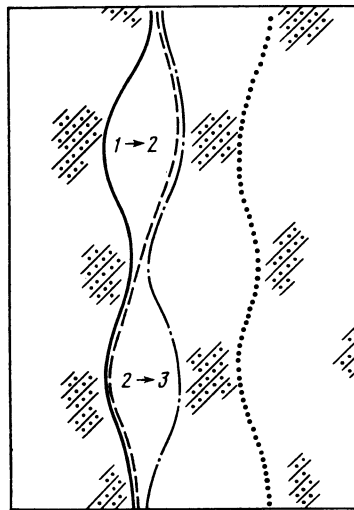


FIG. 6. Sketch illustrating the mechanism of quantum diffusion. Three successive positions of a vortex are shown. The dashed curve depicts the vortex after diffusion has occurred as a result of a sequence of quantum hops by a distance d along the Lorentz line of force; d is roughly equal to the mean distance between adjacent pinning centers (hatched).

netic induction averaged over distances much greater than the coherence length $\xi = (\Phi_0/2\pi H_{c2})^{1/2}$, where Φ_0 is the flux quantum).

In terms of its effects on flux creep, quantum diffusion should be roughly equivalent to additional heating of the specimen (by 1–3 K for $\text{Pb}_{1.2}\text{Mo}_{6.4}\text{S}_8$ specimens with $T_a = 920$ – 1120 °C, for example). This conclusion is also supported by the following estimates.

We start by noting that in this mechanism, vortex tunneling below the barrier is accompanied by energy dissipation. A general method for treating tunneling with “dissipation” was considered recently in Ref. 28. In our case, however, the situation is more complicated because an entire ensemble of interacting quasiparticles (not just a single particle) is involved in the tunneling. One may assume however that after each quantum hop, the most energetic unpaired quasiparticles,¹¹ localized near the core of the vortex, should move a distance equal to the average width $d - 2\xi$ of the energy barrier between adjacent pinning centers. In a superconductor with a mean transport free path l_{tr} , the characteristic time required for quasiparticles with excitation energy $\varepsilon_k > \Delta$ to drift a distance $d - 2\xi$ can be approximated by

$$\tau_d \approx 3(d - 2\xi) / (l_{tr} \xi_0)^{1/2} \langle v_F^* \rangle (1 + \lambda_{e-p}). \quad (5)$$

We now substitute $\lambda_{e-p} = 1.8$ (Ref. 29) for the electron-phonon interaction parameter and use $l_{tr} = 2.3 \cdot 10^{-7}$ cm, $\langle v_F^* \rangle = 4 \cdot 10^6$ cm/s (Ref. 30), and

$$\xi_0 \approx 0.18 (\hbar \langle v_F^* \rangle / k_B T_c) (1 + \lambda_{e-p})$$

for lead molybdenum sulfide; inserting the value $d \approx 3 \cdot 10^{-6}$ cm calculated by Eq. (1) for $\text{Pb}_{1.2}\text{Mo}_{6.4}\text{S}_8$ with $T_a = 1020$ °C, we find $\tau_d \approx 3 \cdot 10^{-12}$ s. The time required for a vortex segment to hop from one quasistable position near a pinning center to another is thus very short; it can be regarded as equivalent to a smearing of the barrier height by an amount $\Delta U \gg \hbar / \tau_d \approx 2.5$ K. The above estimates imply that vortex quantum diffusion should affect flux creep more strongly as the mean distance between pinning centers de-

creases. This is confirmed by comparing the temperature dependences of the flux creep for specimens with various compositions and annealing temperatures.

A more detailed analysis of the effects of vortex quantum diffusion on flux creep would involve an examination of the vortex dynamics and would have to define and calculate the effective mass M_{eff} of a tunneling vortex segment. The vortex dynamics have been analyzed most fully, using various models and computational methods (see, e.g., Refs. 31, 32), for the case of viscous vortex flow, i.e., for relatively strong electric fields $E > 10^{-8}$ V/cm inside the specimen. Because researchers were interested primarily in steady states (for which the drift velocity of the vortex flow V_L is constant), the inert mass of the vortices was naturally neglected.

For much weaker internal fields $E \ll 10^{-8}$ V/cm the vortices are essentially localized; they drift slowly due to repeated hops of local vortex segments, as illustrated in Fig. 6. The use of the viscosity coefficient³¹

$$\eta = 6\alpha\sigma_n\Phi_0 H_{c2}/c^2 = 3\alpha\pi n_0 \hbar^2 \tau_n / m^* \xi^2 \quad (6)$$

to describe such processes is highly problematic in this case. (Here $\alpha = 0.438$, $\sigma_n = n_0 e^2 \tau_n / m^*$ is the specific conductivity of the superconductor in the normal state near the superconducting transition, $\Phi_0 = \pi \hbar c / e$ is the flux quantum, n_0 and m^* are the density and effective mass of the current carriers, respectively, $\tau_n = l_{\text{tr}} / \langle v_F \rangle$ is the relaxation time, and ξ is the coherence length.) Indeed, inertial effects must be considered in order to describe the hopping processes, for which the instantaneous velocity of the core of a vortex segment may change greatly over short times. To draw an analogy, the methods needed to describe the vortex dynamics for the two cases $E > 10^{-8}$ V/cm and $E \ll 10^{-8}$ V/cm should differ in roughly the same way as in the analysis of the carrier kinetics in a normal conducting metal (for which a drift velocity $v_q = \text{const}$ can be introduced, and the corresponding viscosity coefficient is $\eta_q \approx m^* / \tau_n$) as opposed to a material with highly localized carriers, where hopping gives the dominant contribution to the conductivity. Proceeding formally, the viscosity coefficient η (per unit vortex length) should be related to the inert mass M_d of a vortex segment of length l by

$$M_d \approx \eta d \tau_v, \quad (7)$$

where τ_v is the characteristic time of the relaxation processes responsible for irreversible energy dissipation and viscous forces. One can estimate τ_v roughly as follows.

When a perturbation (possibly of fluctuation origin) acts on an individual vortex segment, the generation of normal quasiparticles with characteristic relaxation times $\tau_n \approx \hbar / \epsilon_F$, where ϵ_F is the Fermi energy, is accompanied by hopping of correlated (paired) quasiparticles from the condensate to new energy levels; however, the characteristic relaxation times $\tau_s \approx \hbar / \Delta$ for this process are much longer. It is reasonable to suppose that in a superconductor for which $\xi < d - 2\xi \ll \lambda$, where λ is the penetration depth of the magnetic field, hopping of individual vortex segments from one quasistable position near a pinning center to another adjacent position will be due primarily to diffusion of the most mobile of the normal quasiparticles. The mean Fermi velocity $\langle v_F \rangle$ of the latter is 1–2 orders of magnitude greater than

the maximum pairing rate for the correlated quasiparticles:

$$\langle v_c \rangle \sim \langle v_F \rangle \Delta / \epsilon_F.$$

It is possible for several normal quasiparticles to interact with supercondensate excitations with $\epsilon_k < 2\Delta_m$ localized near a neighboring pinning center,²⁾ where due to the proximity effect the order parameter $|\Delta(r)|$ is generally much less than Δ_m (here Δ_m is the maximum energy gap in the superconductor for a given temperature T , magnetic field H , and transport current density J). This interaction may eventually produce a nonequilibrium redistribution (circulation) of the quasimomentum of hundreds and thousands of paired quasiparticles, thereby redistributing the magnetic induction locally. If the total energy of the normal quasiparticles exceeds a threshold value, the position (spatial configuration) of the vortex segment may change. Since vortex segment hops are accompanied by energy dissipation due to phonon generation and depairing, they can occur only if the potential energy of the vortex decreases. Without going into the factors responsible for the concurrent drifting of the normal quasiparticles in the vortex core along a preferred direction, we may therefore adopt a rough model in which a vortex segment hop over the comparatively short distance $d - 2\xi \ll \lambda$ can be regarded as proceeding in two steps: a rapid movement of the normal core of the vortex followed by relaxation of the order parameter near the new position. In this model, irreversible energy dissipation leading to viscosity effects is due primarily to the interaction of normal particles with excitations and crystal lattice defects; the inert mass of a tunneling vortex segment can therefore be estimated by setting $\tau_v \sim \tau_n$ in (7).

As was shown in Ref. 33, an alternative method for estimating the inert mass of a vortex is provided by the generalized GL theory, in which both the space and the time dependence of the order parameter $\Delta(r, t)$ are considered. It follows from the GL theory that near a localized noninteracting vortex in a type-II superconductor, $\Delta(z, r, \theta)$ increases from zero at the center of the vortex to nearly the maximum value Δ_m at $|r| = \xi(T)$. The rapid change in $|\Delta(r)|$ in the region $r \leq \xi(T)$ can be handled by solving the Bogolyubov equations; one then finds that a group of low-lying excitations with wave functions $v_k(r)$ and $u_k(r)$ is present near the vortex core; the energy levels for some of these excitations are as low as $|\Delta(r)| \sim \Delta_m^2 / \epsilon_F$ (Ref. 34). Because of the energy gap in the excitation spectrum and the interconversion of paired and unpaired quasiparticles, serious difficulties arise when the generalized GL theory is used to analyze time-dependent processes in superconductors in the general case. Indeed, such a treatment is probably feasible only in the linear approximation. However, under suitable restrictions the time-dependent GL equations for the order parameter can in principle be reduced either to the wave equations ($T \rightarrow 0$) or to the diffusion equations ($T \rightarrow T_c$), which contain first-order time and second-order spatial derivatives.^{31,35,36}

Under the assumption that Δ is small in the vortex core ($|r| < \xi$), Suhl showed³³ that in the limit $T \rightarrow 0$ the formula

$$\sum_k \epsilon_k \approx \frac{H_c^2 \xi^2}{8} \approx \frac{\pi \Delta_m^2 n_0}{2 \epsilon_F \xi^2}$$

relating the inert mass to the kinetic energy becomes

$$M_{core} \approx m^* (3\xi^2 H_c^2 / 4m^* \langle v_F \rangle^2) \approx 3m^* \epsilon_F^{-1} \sum_k \epsilon_k \quad (8)$$

where the length of the vortex core is taken as the length unit. If the normal quasiparticles from the vortex core are neglected as was done in Ref. 33, Eq. (8) says that the contribution to the effective vortex mass from supercondensate excitations with $\epsilon_k < 2\Delta_m$ is equivalent to the total mass of a certain number of normal quasiparticles, whose total Fermi energy is roughly three times $\sum \epsilon_k$ in the region $|r| < \xi$.

According to the model discussed above, the tunneling of a vortex segment by a distance $d - 2\xi$ between neighboring pinning centers can be viewed as the propagation of a wave of excitations with $\Delta = 0$. In this wave, the carriers in the superconducting condensate are unpaired particles whose total energy is large enough to ensure that the quasi-momenta of a large number of paired quasiparticles are redistributed, as required for a change in vortex configuration.

Since the total kinetic energy of a noninteracting vortex exceeds the kinetic energy of the core by roughly a factor of $4 \ln(\lambda/\xi)$, it is reasonable to assume that as $T \rightarrow 0$, M_{eff} will exceed the core kinetic energy by roughly the same factor. The energy of the vortex segment increases by $k_B T$ as the temperature rises, and this should contribute further to M_{eff} as some of the paired quasiparticles break up. Since

$$|\Delta(r)|_{min} \approx \Delta_m^2 / \epsilon_F$$

holds near the vortex core,³⁴ the total mass of the normal quasiparticles generated by heating can be estimated by

$$M_n \sim m^* (2k_B T \epsilon_F / \Delta_m^2)^{1/2}.$$

According to Ref. 33, the electromagnetic energy of the vortex could in principle also contribute to M_{eff} ; however, the relative magnitude

$$M_{em} = \frac{1}{3} M_{core} \left(\frac{\lambda}{\xi} \right)^2 \left(\frac{\langle v_F \rangle}{c} \right)^2 \quad (9)$$

of this effect is just a few percent for the superconductors investigated.

The above formulas for M_{eff} yield an estimate for the temperature at which the contributions from thermal activation and from tunneling below the barrier become comparable. Equating the arguments of the exponentials for these two mechanisms, we obtain

$$T \approx \frac{|U_0|_B}{k_B} \left[\left(\frac{8M_{eff}}{\hbar^2} \right)^{1/2} \int_{r_1}^{r_2} U^h(r) dr \right]^{-1}. \quad (10)$$

Here $|U_0|_B$ is the depth of the potential well for a vortex segment of length d near a pinning center,

$$|U(r)| \leq |U_0|_B, \quad |r_2 - r_1| \approx (d - 2\xi).$$

In the Anderson model¹²

$$|U_0|_B = \alpha_0 d_B^4 = \alpha_0 (\Phi_0 / B_0)^2,$$

where the pinning force density $\alpha_0 = 5.5 \cdot 10^8$ dyn/cm³ can be found by extrapolating the curve $\alpha(T)$ to $T \rightarrow 0$ (insert to Fig. 5).

The values of n_0 , m^* , Δ_m , and $\tau_n \approx l_{tr} / \langle v_F \rangle$ in the expression for M_{eff} can be estimated as follows. Hall voltage measurements³⁰ and band calculations³⁷ indicate that the

current carriers in molybdenum sulfide superconductors are "holes," i.e., the conduction band is almost full. For $Pb_{1+x}Mo_{6+y}S_8$, the conduction band contains 21–22 electrons per rhombohedral cell (of volume $V_R \approx a_R^3 \approx 2.8 \cdot 10^{-22}$ cm³). This is 2–3 electrons less than needed to fill the band and form 12 covalent bonds in the Mo_6 octahedron.^{38,39} It follows that the "hole" density in $Pb_{1.2}Mo_{6.4}S_8$ is roughly 10^{22} cm⁻³, in agreement with the value for most other high-temperature superconducting compounds.³⁾

The effective mass of the quasiparticles

$$m^* \approx \hbar \langle k_F \rangle / \langle v_F \rangle,$$

can be estimated, for example, by using the expression in Ref. 40 for the derivative $|dH_{c2}/dT|_{T_c}$. The expression

$$\langle v_F^* \rangle = \langle v_F \rangle / (1 + \lambda_{e-p})$$

for the renormalized mean velocity of the quasiparticles on the Fermi surface, where $\langle v_F \rangle$ is the averaged value of the Fermi band velocity, then becomes

$$\langle v_F^* \rangle = \frac{6\pi k_B c}{7\zeta(3)e} \frac{\eta_{H_{c2}}(T_c)}{l_{tr} R(\lambda_{tr})} \left| \frac{dH_{c2}}{dT} \right|_{T_c}^{-1} (1 + \Lambda^{1/2}), \quad (11)$$

where

$$\Lambda = 1 + \frac{14el_{tr}^2 T_c}{3\hbar c} \frac{R(\lambda_{tr}) \zeta(3)}{\eta_{H_{c2}}(T_c)} \left| \frac{dH_{c2}}{dT} \right|_{T_c},$$

$$\eta_{H_{c2}}(T_c) = 1 + (\pi T_c / \omega_0)^2 (0.6 \ln \omega_0 / T_c - 0.26), \quad \zeta(3) = 1.202;$$

the parameter

$$R(\lambda_{tr}) = R(\hbar \langle v_F \rangle / 2\pi k_B T l_{tr})$$

increases monotonically with λ_{tr} from $R(0) = 1$ to $R(\infty) = \pi^2 [7\zeta(3)]^{-1} = 1.17$. The transport mean free path in ternary molybdenum sulfides is usually estimated by³⁰

$$l_{tr} \sim a_R \rho_{max} / \rho_n \sim 1.5 a_R \rho_{300 K} / \rho_n$$

where $a_R = 6.5 \cdot 10^{-8}$ cm is the rhombohedral cell parameter. Inserting the values $|dH_{c2}/dT|_{T_c} = 50$ kOe/K, $l_{tr} = 2 \cdot 10^{-7}$ cm, $T_c = 12.7$ K, and $\omega_0 \approx 50$ K for a $Pb_{1.2}Mo_{6.4}S_8$ specimen annealed at 1020 °C, we find $\langle v_F^* \rangle = 5.9 \cdot 10^6$ cm/s.

If we assume, as we did in using (11), that the "hole" pockets in the Fermi surface are approximately spherical for the $Pb_{1.2}Mo_{6.4}S_8$ system, which is nearly cubic (the rhombohedral angle α_R is $89.41^\circ \approx 90^\circ$), we get

$$\langle k_F \rangle = (3\pi^2 n_0)^{1/3} = 6.7 \cdot 10^7 \text{ cm}^{-1},$$

whence $m^* = \hbar \langle k_F \rangle / \langle v_F \rangle \approx 4.2 \cdot 10^{-27} g \approx 4.6 m_e$. This value is large because in these compounds the d -states give the dominant contribution to the superconductivity (and to the conductivity).³⁷

With the above estimates for m^* , n_0 , $\tau_n \approx l_{tr} / \langle v_F \rangle \approx 1.2 \cdot 10^{-14}$ s, and $d \approx 3 \cdot 10^{-6}$ cm for a $Pb_{1.2}Mo_{6.4}S_8$ specimen with $T_a = 1020$ °C, Eqs. (6) and (7) give

$$M_d \approx 3\alpha \pi n_0 \hbar^2 \tau_n^2 d / m^* \xi^2 \approx 5 \cdot 10^{-26} g \approx 12 m^*.$$

This result is in satisfactory agreement with the estimate

$$M_{eff} \approx m^* \left[6\pi n_0 \xi^2 d \left(\frac{\Delta_m}{\epsilon_F} \right)^2 \left(\frac{1}{4} + \ln \frac{d}{2\xi} \right) + \left(\frac{2k_B T \epsilon_F}{\Delta_m^2} \right)^{1/2} \right] \approx 11 m^*$$

for $T = 3$ K obtained from energy arguments as in Ref. 33.

However, in addition to the kinetic energy of the vortex core, it includes the kinetic energy of the correlated quasiparticles in the region $\xi < |r| < 0.5d$ and allows for the normal quasiparticles from the vortex core when $\xi < d - 2\xi \ll \lambda$ and $T < 0.5T_c$. The mass M_{eff} at $T = 3$ K estimated in this way is some 20 times greater than M_{core} (Ref. 33).

Inserting M_{eff} into (10), we find that quantum tunneling should contribute about as much to flux creep as the activation mechanism for $T \approx 2.5$ –3 K. This estimate agrees closely with the experimental data (Fig. 3) and with the smearing $\Delta U \approx 2.5$ K of the energy barrier height estimated using (5).

Our estimates thus show that the agreement between the experimental data and the theoretical results on vortex dynamics with weak energy dissipation can be improved substantially by treating the contribution from quantum tunneling to the diffusion of the vortices. The quantum diffusion should influence the flux creep more strongly as the temperature and the mean distance between pinning centers decrease. This is confirmed by comparing the temperature dependences of the flux creep for specimens with different compositions and annealing temperatures.

Quantum diffusion of vortices might also explain the abrupt rise in $J_c(T)$ when T decreases by 2–3 K relative to the extrapolated values $T_c(J_c \rightarrow 0)|_{H=\text{const}}$. Further studies of specimens with different microstructures over a wider range of temperature and magnetic and electric fields should yield more detailed information about the contribution of vortex quantum diffusion to the relaxation processes, current characteristics, and other properties of superconducting systems.

CONCLUSIONS

Our data indicate that except for initial times $t < 20$ s, the “frozen” field H_i decays logarithmically with t for all of the ternary molybdenum sulfides investigated, for which J_c at $H = 10$ kOe and $T = 4.2$ K was greater than 10^4 A/cm². Although $H_i(t)$ continued to decay logarithmically when T dropped from 4.2 to 0.5 K, the flux creep rate was observed to fall off much more slowly than predicted by treatments based solely on the activation mechanism.¹² It was shown that quantum diffusion of vortices must be considered in order to resolve this discrepancy. Our estimates show that the contributions to flux creep from quantum diffusion and thermal activation are roughly equal for $T = 1.5$ –3 K.

Analysis of the data shows that as the temperature and mean distance between neighboring pinning centers decrease, the relative contribution to vortex diffusion from tunneling beneath the barrier increases.

Our model, which treats both thermal activation and quantum diffusion, predicts that in type-II superconductors with a high density of effective pinning centers, the induced current J_c should be “damped” appreciably even for very low temperatures $T \rightarrow 0$, provided the average induction in the specimen exceeds H_{c1} . Further studies of type-II superconductors with ordered microstructures are needed to obtain more detailed information on the dynamics of the vortex lattice.

I am grateful to N. E. Alekseevskii and V. I. Inzhankovskii for helpful comments in a discussion of these results, and to E. P. Khlybov for carrying out the x-ray analysis of the phase compositions.

¹Andreev reflection is negligible for quasiparticles with excitation energy $\epsilon_k > \Delta \approx 2k_B T_c$.

²We deal with strong pinning centers, for instance inclusions of nonsuperconducting phases with characteristic dimensions $\sim \xi$.

³The Hall data lead to estimates $n_0 = (3-7) \cdot 10^{22}$ cm⁻³ (Ref. 30) for the carrier density. These values are somewhat too high, because one is not justified in using the Drude formula $R_H = -(n_0 e c)^{-1}$ in the single-band approximation which, as is well known, is accurate only for the alkali metals.

⁴S. Foner, E. J. McNiff Jr., and E. J. Alexander, Phys. Lett. A **49**, 269 (1974).

⁵O. Fischer, M. Decroux, S. Roth, R. Chevrel, and M. Sargent, J. Phys. C **8**, L474 (1975).

⁶N. E. Alekseevskii, A. V. Mitin, Ch. Bazan, N. M. Dobrovol'skii, and B. Ronchka, Zh. Eksp. Teor. Fiz. **74**, 384 (1978) [Sov. Phys. JETP **47**, 199 (1978)].

⁷N. E. Alekseevskii, N. M. Dobrovol'skii, D. Ékkert, and V. I. Tsebro, Zh. Eksp. Teor. Fiz. **72**, 1145 (1977) [Sov. Phys. JETP **45**, 599 (1977)].

⁸N. E. Alekseevskii, A. V. Mitin, and E. P. Khlybov, Zh. Eksp. Teor. Fiz. **82**, 927 (1982).

⁹V. R. Karasik, E. V. Karyayev, M. O. Rikel', and V. I. Tsebro, Zh. Eksp. Teor. Fiz. **83**, 1529 (1982) [Sov. Phys. JETP **56**, 881 (1982)].

¹⁰C. Rossel and O. Fischer, J. Phys. F **14**, 455 (1984).

¹¹N. E. Alekseevskii, V. V. Evdokimova, A. V. Mitin *et al.*, Fiz. Met. Metalloved. **59**, 900 (1985).

¹²N. E. Alekseevskii, M. Glinskii, N. M. Dobrovol'skii, and V. I. Tsebro, Pis'ma Zh. Eksp. Teor. Fiz. **23**, 455 (1976) [JETP Lett. **23**, 412 (1976)].

¹³S. A. Alterovitz, J. A. Woollam, L. Kammerdiner, and H. L. Luo, Appl. Phys. Lett. **33**, 264 (1978).

¹⁴K. Hamasaki, T. Inoue, T. Yamashita, and T. Komata, Appl. Phys. Lett. **41**, 667 (1982).

¹⁵P. W. Anderson, Phys. Rev. Lett. **9**, 309 (1962).

¹⁶Y. B. Kim, C. F. Hempstead, and A. R. Strnad, Phys. Rev. Lett. **9**, 306 (1962).

¹⁷Y. B. Kim, C. F. Hempstead, and A. R. Strnad, Phys. Rev. **131**, 2486 (1963); R. D. Dunlap, C. F. Hempstead, and Y. B. Kim, J. Appl. Phys. **34**, 3147 (1963).

¹⁸M. R. Beasley, R. Labusch, and W. W. Webb, Phys. Rev. **181**, 682 (1969).

¹⁹J. M. A. Wade, Phil. Mag. **20**, 1107 (1969).

²⁰M. Polak, I. Hlasic, and L. Krempasky, Cryogenics **13**, 702 (1973).

²¹H. Boesch, B. Lischke, and H. Sollig, Phys. Stat. Sol. (b) **61**, 215 (1974).

²²G. Antesberger and H. Ullmaier, Phil. Mag. **29**, 1101 (1974).

²³J. E. Nicholson, R. S. Cort, and G. P. Cort, J. Low Temp. Phys. **26**, 69 (1977).

²⁴H. R. Kerchner, J. Low Temp. Phys. **34**, 33 (1978).

²⁵L. Miu and S. Popa, J. Low Temp. Phys. **42**, 203 (1981).

²⁶N. E. Alekseevskii and A. V. Mitin, Fiz. Met. Metalloved. **50**, 1179 (1980).

²⁷N. E. Alekseevskii, Zh. Eksp. Teor. Fiz. **8**, 1098 (1938).

²⁸C. P. Bean, Phys. Rev. Lett. **8**, 250 (1962).

²⁹G. L. Dorofeyev, A. B. Imenitov, and E. Yu. Klimenko, Cryogenics **20**, 307 (1980).

³⁰E. Yu. Klimenko and A. E. Trenin, Cryogenics **23**, 527 (1983).

³¹Yu. Kagan and N. V. Prokof'ev, Pis'ma Zh. Eksp. Teor. Fiz. **43**, 434 (1986) [JETP Lett. **43**, 558 (1986)].

³²N. E. Alekseevskii, N. M. Dobrovol'skii, H. Wolf, and H. Holfeld, Zh. Eksp. Teor. Fiz. **83**, 1500 (1982) [Sov. Phys. JETP **56**, 865 (1982)].

³³J. A. Woollam and S. A. Alterovitz, Phys. Rev. B **19**, 749 (1979).

³⁴L. P. Gor'kov and N. B. Kopnin, Usp. Fiz. Nauk **116**, 413 (1975) [Sov. Phys. Usp. **18**, 496 (1975)].

³⁵S. Imai, Prog. Theor. Phys. Jpn. **54**, 624 (1975).

³⁶H. Suhl, Phys. Rev. Lett. **14**, 226 (1965).

³⁷J. Bardin, R. Klimmel, A. E. Jacobs, and L. Tewordt, Phys. Rev. **187**, 556 (1969).

³⁸E. Abrahams and T. Tsuneto, Phys. Rev. **152**, 416 (1966).

³⁹L. P. Gor'kov and G. M. Éliashberg, Zh. Eksp. Teor. Fiz. **54**, 612 (1968) [Sov. Phys. JETP **27**, 328 (1968)].

⁴⁰D. W. Bullitt, Phys. Rev. Lett. **39**, 664 (1977); T. Jarlborg and A. J. Freeman, Phys. Rev. Lett. **44**, 178 (1980); O. K. Anderson, W. Klose, and H. Nohl, Phys. Rev. B **17**, 1209 (1978).

⁴¹A. M. Umarji, G. V. S. Rao, M. P. Janawadkar, and T. S. Radhakrishnan, Sol. St. Commun. **37**, 1 (1981).

⁴²K. Yvon and A. Paoli, Sol. St. Commun. **24**, 41 (1977).

⁴³T. P. Orlando, E. J. McNiff Jr., S. Foner, and M. R. Beasley, Phys. Rev. B **19**, 4545 (1979).

Translated by A. Mason